Characterization of three LYSO crystal batches

Fan Yang *, Rihua Mao, Liyuan Zhang, Ren-Yuan Zhu

256-48, HEP, California Institute of Technology, Pasadena, CA 91125, USA

ARTICLE INFO

ABSTRACT

We report on three LYSO crystal batches characterized at the Caltech crystal laboratory for future HEP experiments: 25 20 cm long crystals for the SuperB experiment; 12 13 cm long crystals for the Mu2e experiment and 623 $14 \times 14 \times 1.5$ mm^3 plates with five holes for a LYSO/W Shashlik matrix for a beam test at Fermilab. Optical and scintillation properties measured are longitudinal transmittance, light output and FWHM energy resolution. Correlations between these properties are also investigated.

© 2014 Elsevier B.V. All rights reserved.

1. Introduction

Because of their high density (7.4 g/cm^3), short radiation length (1.14 cm), fast (40 ns) and bright (4 times BGO) scintillation, cerium doped lutetium oxyorthosilicate (Lu_2SiO_5:Ce, LSO) [1–5] and lutetium yttrium oxyorthosilicate ($Lu_{2(1-x)}Y_{2x}SiO_5$:Ce, LYSO) [6–8] crystals have attracted a broad interest in the high energy physics community pursuing a precision electromagnetic calorimeter for future high energy physics experiments [9–13]. Their excellent radiation hardness against gamma-rays [14,15], neutrons [16] and charged hadrons [17] also makes them a preferred material for calorimeters to be operated in a severe radiation environment, such as the HL-LHC.

All crystal vendors are encouraged to provide crystals for future HEP experiments. The choice of vendors will be made in each experiment based upon cost and performance. It is the hope that the paper is useful for crystal vendors to improve the quality of their crystals. Fig. 1 shows 25 20 cm long LYSO crystals of tapered geometry with about 20×20 mm^2 at the small end and 23×23 mm^2 at the large end for the SuperB experiment. They were grown by the Czochralski method at Saint-Gobain (SG) Corporation, Shanghai Institute of Ceramics (SIC) and Sichuan Institute of Piezo-electric and Acousto-optic Technology (SIPAT). Fig. 2 shows 10 rectangular Mu2e crystals with dimension of $30 \times 30 \times 130$ mm^3 and other two hexagonal crystals 18.6 mm wide and 130 mm long. All the Mu2e crystals were grown at SIC. Fig. 3 shows 623 $14 \times 14 \times 1.5$ mm^3 LYSO plates grown at SIC for a LYSO/W Shashlik matrix [11]. There are five holes in these plates to allow four wavelength shifters and one monitoring fiber to go through. All six faces of these crystals are polished.

The longitudinal transmittance (LT) was measured using a PerkinElmer LAMBDA 950 UV/vis spectrophotometer with double beam, double monochromator and a large crystal compartment equipped with an integrating sphere. The systematic uncertainty in repeated measurements is 0.15%. The scintillation light output (LO) of SuperB crystals was measured by using a pair of Hamamatsu S8664-55 APDs because the SuperB project chose APD as the photo-detector. Their FWHM energy resolution (ER) was measured by a Hamamatsu R1306 PMT with a bi-alkali photocathode and a borosilicate glass window because the noise contribution APD readout is not adequate for the ER measurement in laboratory with radioactive sources. The scintillation LO and ER were also measured by the Hamamatsu R1306 PMT for Mu2e crystals and Shashlik plates. In the LO measurement for long crystals the large (tapered crystals) or one (rectangular and hexagonal crystals) end of the crystals was coupled to the PMT with Dow Corning 200 fluid, while all other faces of the crystal were wrapped with Tyvek paper. A ^{22}Na source was used to excite the crystals, and provided the coincidence trigger. In the LO measurement for LYSO plates, one large face was coupled to the PMT with an air gap, while all other faces were wrapped with Tyvek paper. A ^{137}Cs source was used to excite the crystals. The γ-ray peak positions were obtained by a simple Gaussian fit. The systematic uncertainty in repeated measurements is less than 1%. Systematic uncertainties of our measurement were defined as RMS/mean of 10 measurements for the same sample.

2. Properties of long LYSO crystals for the SuperB and Mu2e experiments

2.1. Longitudinal transmittance and emission weighted longitudinal transmittance

Fig. 4 shows the LT at 420 nm for the SuperB LYSO crystals with divergences of less than 2% for crystals produced by each vendor,

* Corresponding author.
E-mail address: zhu@hep.caltech.edu (R.-Y. Zhu).
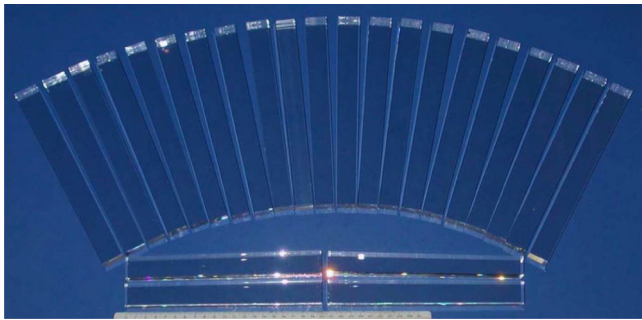
Fig. 1. Twenty five 20 cm long LYSO crystals of tapered shape for SuperB.

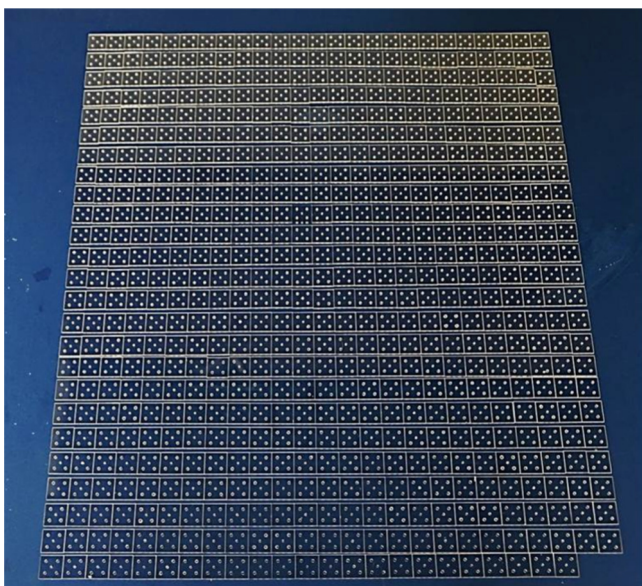**Fig. 2.** Twelve 13 cm long LYSO crystals for Mu2e.

Fig. 3. 623 $14 \times 14 \times 1.5$ mm^3 LYSO plates for a LYSO/W Shashlik matrix.
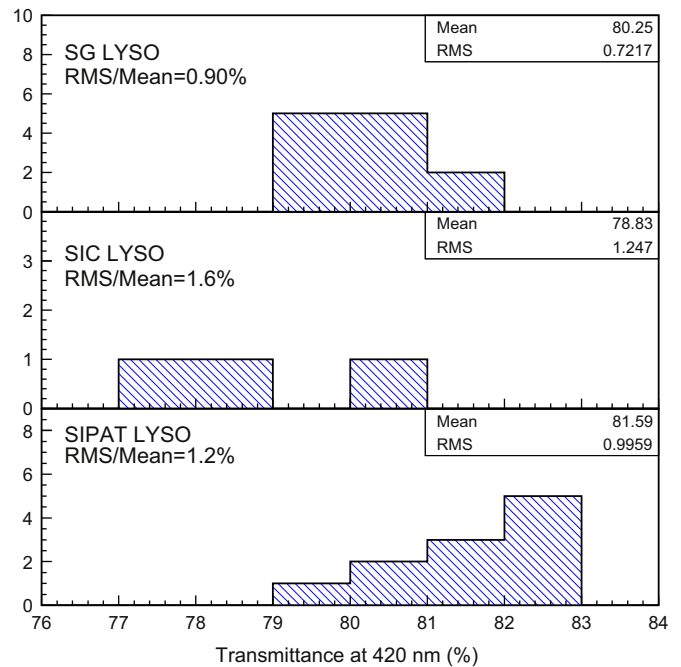

Fig. 4. LT at 420 nm measured for 25 SuperB LYSO crystals.

where 420 nm was chosen since the emission peak of LYSO crystals excited by gamma-rays is at 420 nm [18]. The LO of LYSO crystals is related to the LT at 420 nm. Therefore the LT at 420 nm is essential to the crystal quality control. Among three vendors SIPAT crystals have better average LT at 420 nm. Fig. 5 shows the LT at 420 nm for the Mu2e LYSO crystals. Rectangular and hexagonal crystals have consistent LT with an overall divergence of less than 1%, where two crystals of different shapes cut from the same ingot are shaded with red color. All crystals have LT at 420 nm better than the 75% specification, indicating good optical quality.

Figs. 6 and 7 show emission weighted longitudinal transmittance (EWLT) for SuperB and Mu2e crystals respectively, where EWLT is defined as [9]

$$EWLT = \frac{\int LT(\lambda)Em(\lambda)d\lambda}{\int Em(\lambda)d\lambda} \qquad (1)$$

EWLT presents crystal transmittance in the entire emission spectrum so it is a better representation for crystal's transparency than the transmittance at 420 nm. Fig. 6 shows that crystals grown at Saint-Gobain and SIPAT have better EWLT than that from SIC. Fig. 7 shows that the rectangular and hexagon crystals have consistent EWLT, where two crystals cut from the same ingot are shaded with red color. A larger divergence for EWLT than the LT at 420 nm was observed since EWLT is affected by both transmittance and the UV cutoff wavelength, which is affected by the cerium concentration in the crystal [6]. A small divergence at a level of 1.7% was observed for the Saint-Gobain crystals as well as the Mu2e SIC crystals, indicating consistent cerium doping in these batches.

### 2.2. Light output and FWHM energy resolution

Fig. 8 shows the LO measured by a pair of Hamamatsu S8664-55 APDs for 25 SuperB LYSO crystals. While the SIPAT crystals have the best LO among three vendors, the Saint-Gobain crystals have the best consistency at about 3%. Fig. 9 shows the LO measured by the Hamamatsu R1306 PMT with a divergence of less than 6% for 12
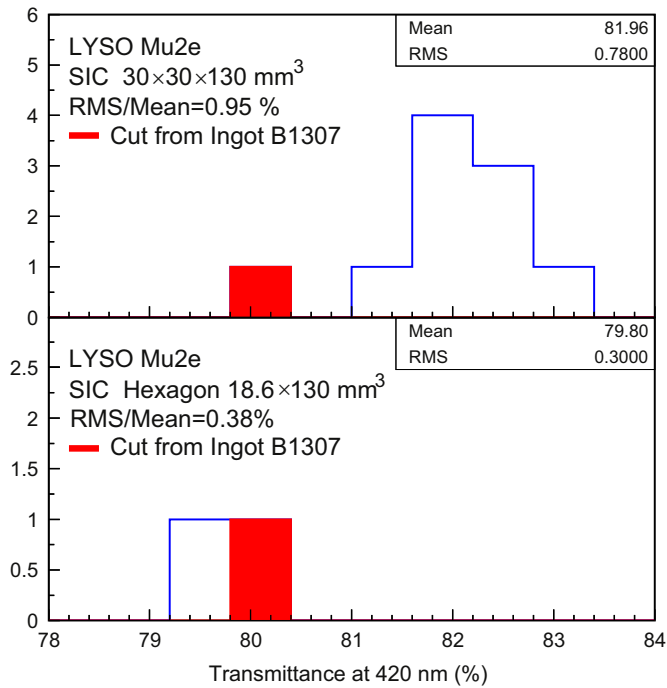
Fig. 5. LT at 420 nm measured for 12 Mu2e LYSO crystals. (For interpretation of the references to color in this figure, the reader is referred to the web version of this article.)
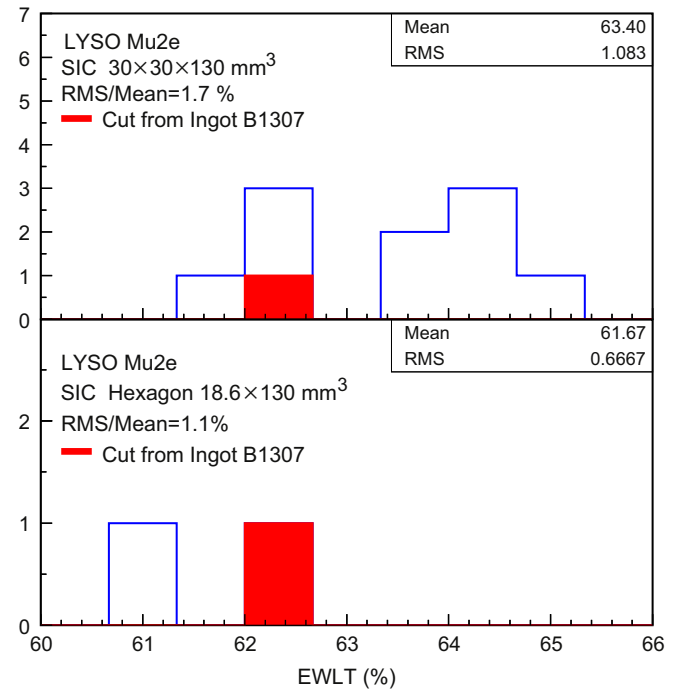
Fig. 7. EWLT measured for 12 Mu2e LYSO crystals. (For interpretation of the references to color in this figure, the reader is referred to the web version of this article.)
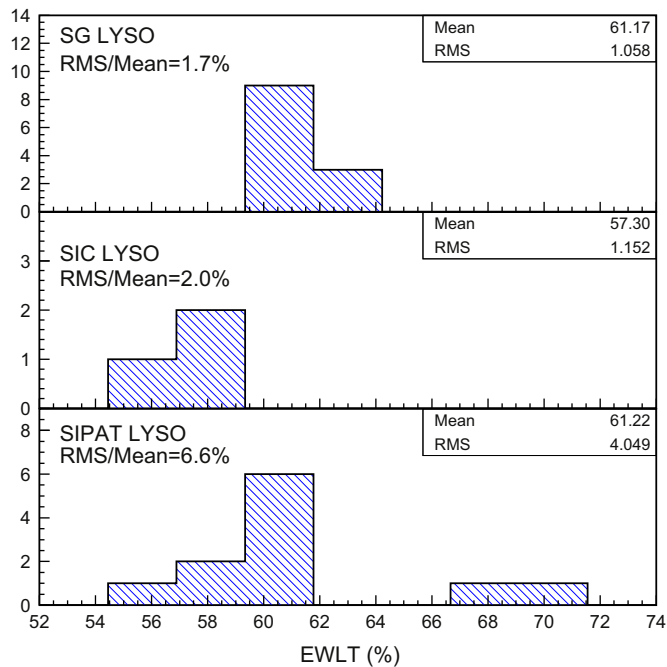
Fig. 6. EWLT measured for 25 SuperB LYSO crystals.
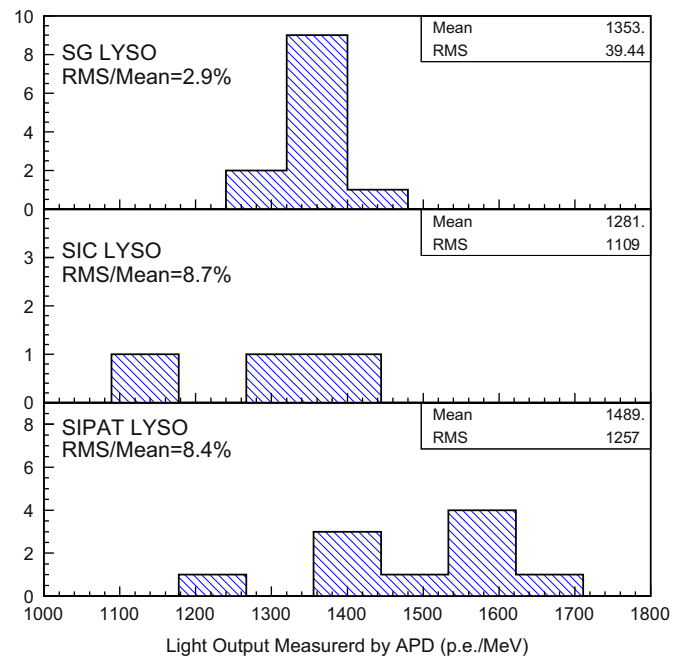
Fig. 8. LO measured by APD for 25 SuperB LYSO crystals.

Mu2e crystals. The rectangular crystals appear to have higher LO than hexagonal ones cut from the same ingot. Further investigation, including a detailed ray-tracing simulation, however, is needed to understand this difference.

Fig. 10 shows the FWHM ER measured by the Hamamatsu R1306 PMT for 25 SuperB crystals excited by 511 keV gamma rays. The Saint-Gobain crystals have the best ER with a divergence of less than 2%. Fig. 11 shows the FWHM ER measured by the Hamamatsu R1306 PMT for 12 Mu2e crystals excited by 511 keV gamma rays. Consistent

ER between the rectangular and hexagonal crystals is observed. The ER divergence of SuperB LYSO is less than that of LO. It is due to the different readout devices in the ER and LO measurements. The ER of SuperB LYSO was measured by the Hamamatsu R1306 PMT and LO was measured by a pair of Hamamatsu S8664-55 APDs. The noise of APD is larger than that of PMT. Because of the noise contribution, APD readout shows higher ER divergence of SuperB LYSO. The ER and LO of Mu2e LYSO were measured by the Hamamatsu R1306 PMT and consistent divergence was observed in rectangular Mu2e LYSO.

2.3. Correlations between the optical and scintillation properties

Fig. 12 shows a slight correlation observed between the LO and the LT at 420 nm for 25 SuperB crystals. Also shown in the figure is the corresponding linear correlation coefficients (CC), defined as [13]

$$CC = \frac{\sum(x-\bar{x})(y-\bar{y})}{\sqrt{\sum(x-\bar{x})^2\sum(y-\bar{y})^2}} \qquad (2)$$

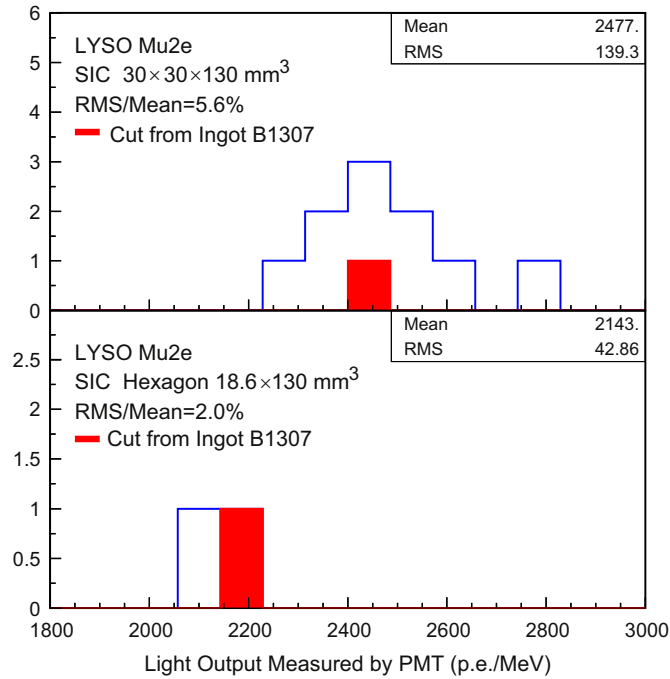Fig. 13 shows a higher positive correlation coefficient at 74% observed between the LO and the LT at 420 nm for 12 Mu2e crystals than 40% observed for the SuperB crystals because of single crystal vendor. This positive correlation indicates that LO of long LYSO crystals is affected by their optical transparency through a light propagation process in the crystal. Fig. 14 shows a strong positive correlation at 90% observed between the LO and the decay time for 12 Mu2e crystals. This positive correlation indicates that
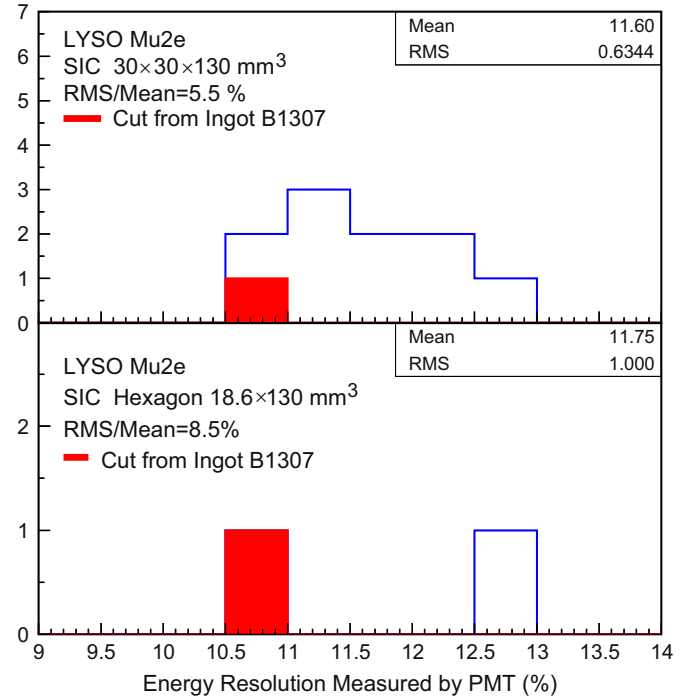

Fig. 9. LO measured by PMT for 12 Mu2e LYSO crystals.

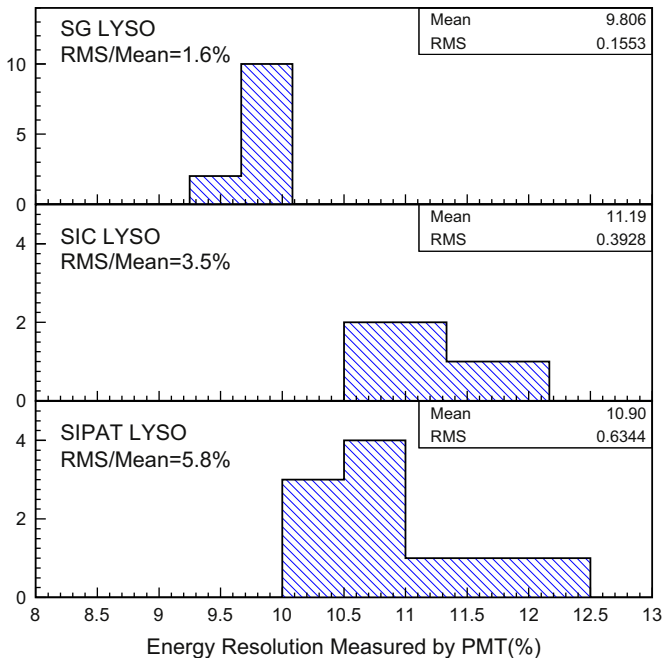**Fig. 11.** ER measured by PMT for 12 Mu2e LYSO crystals.

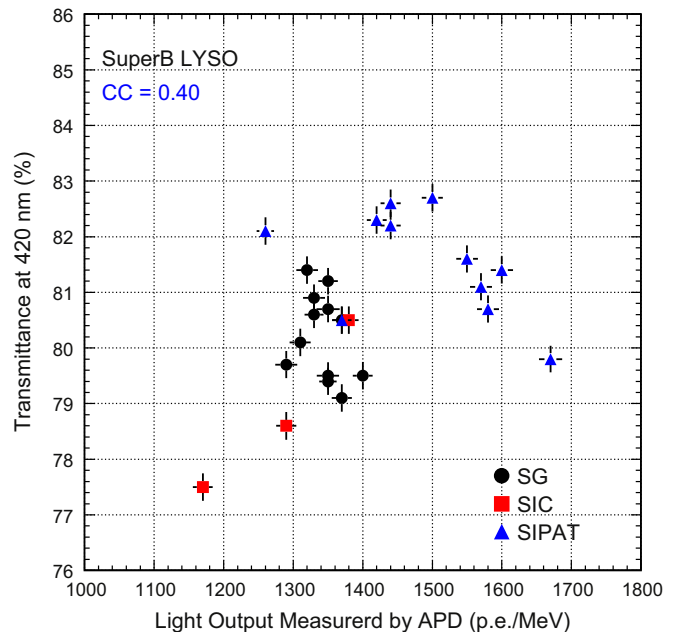**Fig. 10.** ER measured by PMT for 25 SuperB LYSO crystals.

Fig. 12. Correlation between the LO and the LT at 420 nm of 25 SuperB crystals.

the decay time obtained by fitting the light output as a function of the integration time is affected by the light propagation in the crystal.

3. Properties of LYSO plates for a LYSO/W Shashlik test beam matrix

Fig. 15 shows the LO measured by the Hamamatsu R1306 PMT for 623 LYSO plates for a LYSO/W Shashlik test beam matrix [11]. The plates can be divided into two groups according to their LO. While the high peak shows 3284 p.e./MeV with a divergence of

3.6%, the 15% lower peak shows 2793 p.e./MeV with a divergence of 3.2%. Plates in these two groups are actually from different ingots according to the manufacture. Fig. 16 shows the FWHM ER measured for all plates, which can also be divided into two groups. The average ER value of the better group is 9.1% with divergence of 6.6% and that of the other group is 11.6% with divergence of 7.0%. Fig. 17 shows a negative correlation between the light output and the energy resolution as expected.

Fig. 18 shows very consistent transmittance at 420 nm for all LYSO plates except two with significantly lower transmittance. Fig. 19 shows no correlation between the LO and the transmittance
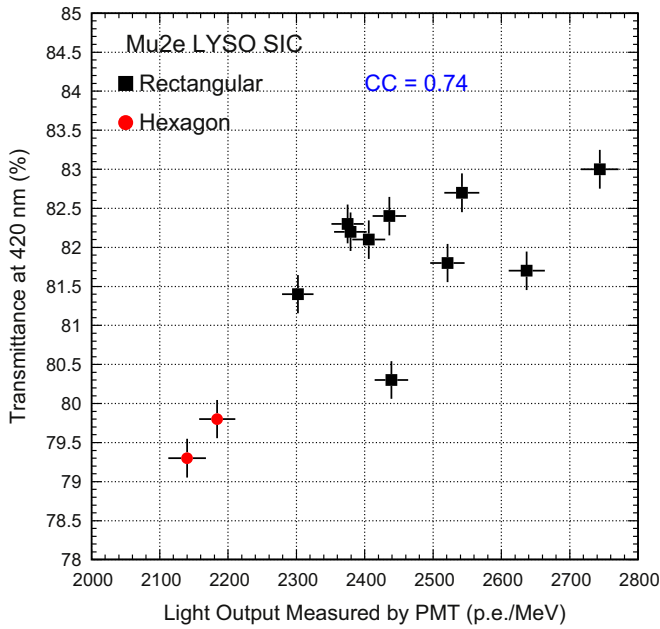

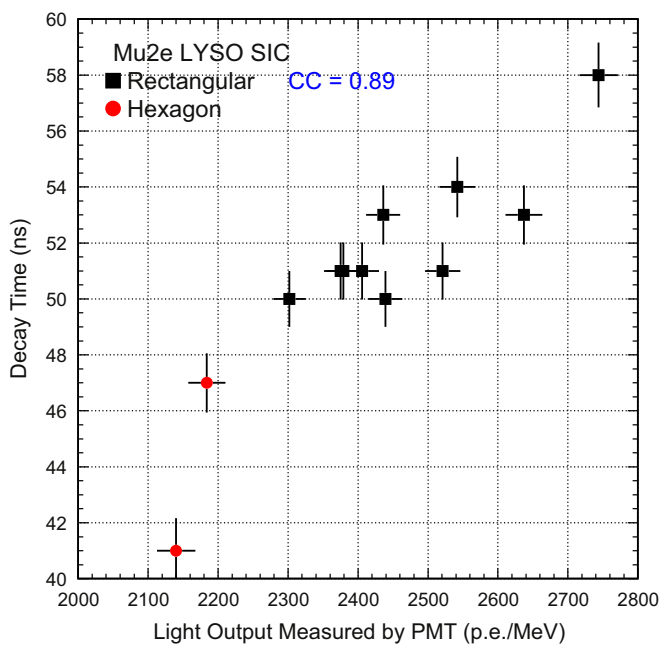**Fig. 13.** Correlation between the LO and the LT at 420 nm of 12 Mu2e crystals.

Fig. 15. LO of 623 LYSO plates for a Shashlik matrix.

Fig. 14. Correlation between the LO and the decay time of 12 Mu2e crystals.
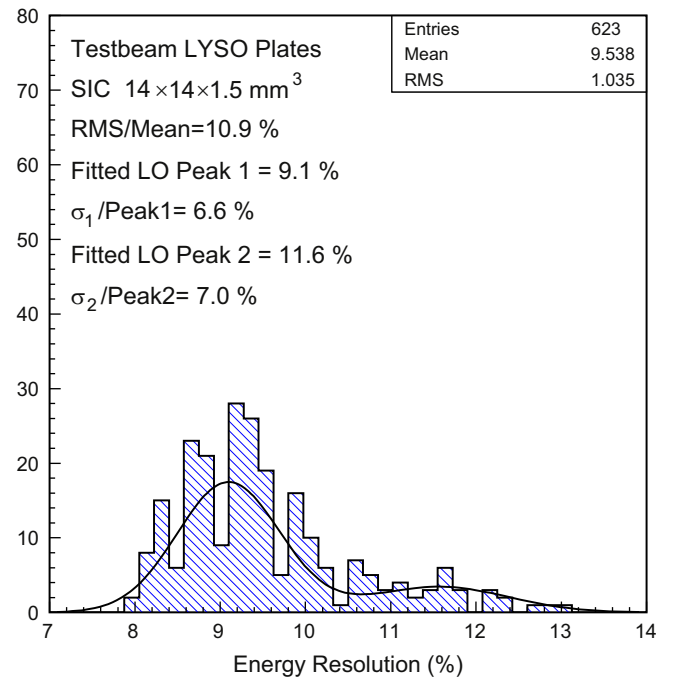

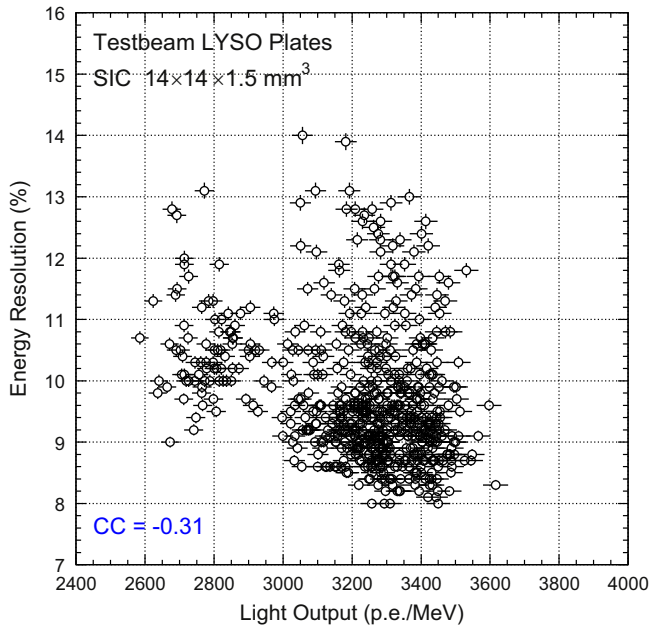**Fig. 16.** ER of 623 LYSO plates for a Shashlik matrix.

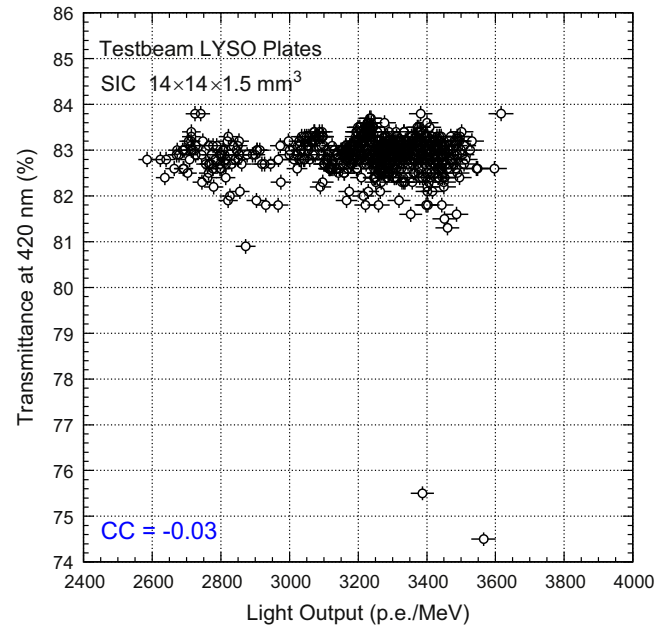**Fig. 17.** Correlation between the LO and the ER of 623 plates.

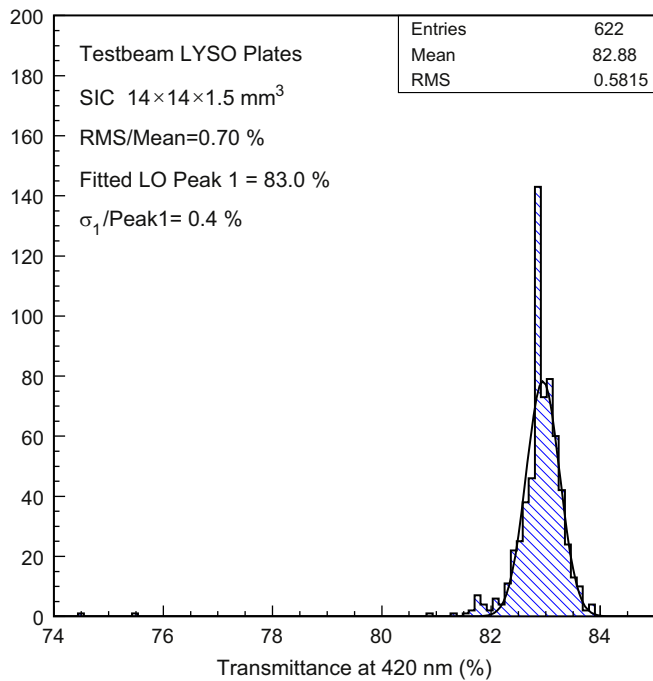**Fig. 19.** Correlation between the LO and the transmittance at 420 nm of 623 plates.

Fig. 18. Transmittance at 420 nm is shown for LYSO plates for a Shashlik matrix.

at 420 nm for these plates, indicating that the measured transmittance has negligible effect on the LO.

4. Summary

Long LYSO crystals produced in industry show good transmittance exceeding 75% specification at 420 nm and good FWHM energy resolution better than 12.5% specification at 511 keV. Typical LO spread is at a level of 6% for long crystals, which may be reduced to about 3% in mass production. Correlations are observed between the LO and the LT at 420 nm as well as between LO and decay time for long LYSO crystals. A slight anti-correlation was observed between the LO and the energy resolution for $14 \times 14 \times 1.5$ mm^3 LYSO plates. Results of these investigations indicate that the quality of LYSO crystals grown in industry is adequate for future HEP calorimeters at both the energy and intensity frontiers.

References

[1] C.L. Melcher, J.S. Schweitzer, IEEE Transactions on Nuclear Science NS-39 (1992) 502.
[2] C.L. Melcher, J.S. Schweitzer, Nuclear Instruments and Methods in Physics Research Section A 314 (1992) 212.
[3] M. Kobayashi, M. Ishii, C.L. Melcher, Nuclear Instruments and Methods in Physics Research Section A 335 (1993) 509.
[4] F. Daghighian, P. Shenderov, K.S. Pentlow, M.C. Graham, B. Eshaghian, C.L. Melcher, et al., IEEE Transactions on Nuclear Science NS-40 (1993) 1045.
[5] G.H. Ren, S.H. Wang, H.Y. Li, S. Lu, Journal of Inorganic Materials 18 (2003) 269.
[6] T. Kimble, M. Chou, B.H.T. Chai, Proceedings of the IEEE Nuclear Science Symposium Conference, 2002, Norfolk, Virginia, USA, vol. 3, p. 1434.
[7] D.W. Cooke, K.J. McClellan, B.L. Bennett, J.M. Roper, M.T. Whittaker, R.E. Muenchausen, et al., Journal of Applied Physics 88 (2000) 7360.
[8] I. Vilardi, A. Braem, E. Chesi, F. Ciocia, N. Colonna, F. Corsi, et al., Nuclear Instruments and Methods in Physics Research Section A 564 (2006) 506.
[9] J.M. Chen, R.H. Mao, L.Y. Zhang, R.Y. Zhu, IEEE Transactions on Nuclear Science NS-54 (2007) 718.
[10] J.M. Chen, L.Y. Zhang, R.Y. Zhu, IEEE Transactions on Nuclear Science NS-52 (2005) 3133.
[11] L.Y. Zhang, R.H. Mao, F. Yang, R.Y. Zhu, IEEE Transactions on Nuclear Science NS-61 (2014) 483.
[12] G. Eigen, Z. Zhou, D. Chao, C.H. Cheng, B. Echenard, K.T. Flood, et al., Nuclear Instruments and Methods in Physics Research A 718 (2013) 107.
[13] SuperB Conceptual Design Report, INFN/AE-07/2, SLAC-R-856, LAL 07-15, March 2007.
[14] J.M. Chen, R.H. Mao, L.Y. Zhang, R.Y. Zhu, IEEE Transactions on Nuclear Science NS-54 (2007) 1319.
[15] R.H. Mao, L.Y. Zhang, R.Y. Zhu, IEEE Transactions on Nuclear Science NS-59 (2012) 2224.
[16] L.Y. Zhang, R.H. Mao, R.Y. Zhu, Proceedings of the IEEE Nuclear Science Symposium Conference, 2009, Orlando, Florida, USA, p. 2041.
[17] G. Dissertori, D. Luckey, F. Nessi-Tedaldi, F. Pauss, M. Quittnat, R. Wallny, et al., Nuclear Instruments and Methods in Physics Research Section A 745 (2014) 1.
[18] R.H. Mao, L.Y. Zhang, R.Y. Zhu, IEEE Transactions on Nuclear Science NS-55 (2008) 1759.